

Structural Optimization of the AISHa Ion Source

F. Noto^{1*}, M. Piscopo¹, L. Celona¹, D. Cittadino¹, S. Gammino¹, G. Cuttone¹,
G. Gallo¹, G. Schillaci¹, C. Campisano², L. Lo Nigro³, G. Costa³, A. Campisano⁴

¹ Laboratorio Nazionale del Sud, Santa Sofia, Catania, Italy

² HITECH 2000, Gravina di Catania, Sicily, Italy

³ C3 S.R.L., Trinacria, Canalicchio, Catania, Italy

⁴ Unico Informatica, Via delle Rose, Sant'Agata, li Battiati, Catania, Italy

*Corresponding author: Francesco Noto, Via Santa Sofia 64, 95123, Catania, ITALY, francesco.noto@lns.infn.it

Abstract: Several facilities for hadron therapy have been built or designed in the recent past and Italy is present in the field with both synchrotron-based and cyclotron-based facilities. For both types of accelerators the availability of high brightness multiply charged ion beams is essential and R&D efforts in this subject are increasing. Optimization of beam emittance and intensity is of primary importance to obtain the necessary current in the RFQ-LINAC, and future facilities may require much better performances in terms of beam brightness than the ones provided by commercial ECRIS.[1]

The design of a relatively compact ECR ion source operating at 18 GHz, named AISHa, has been studied recently. The AISHa ion source has been designed by keeping in mind the typical requirements of hospital-based facilities, where the minimization of the mean time between failures (MTBF) is a key point together with the maintenance operations which should be fast and easy. Some critical parts of the facilities, the plasma chamber, the containment chamber, etc., have been studied and optimized with the COMSOL software.

In conclusion we have studied in particular the plasma chamber under certain imposed conditions: the chamber needs to be cooled by water, which flows in a given path to be reached through an entrance and septa.

Keywords: Hadron therapy, CFD.

1. Introduction

During the '90s different ion sources have been built at INFN-LNS, two for the production

of highly charged heavy ions to be accelerated by the K-800 Superconducting Cyclotron [2,3]. In the recent past, the requests have been more and more relevant either in terms of beam current or in terms of highly charged ion beams from metallic samples, so a decision to update the existing hardware to fulfil the new needs and to improve the two sources has been taken and the first steps have been done.

The AISHa source for hadron therapy facilities is designed for high brightness multiply charged ion beams with high reliability, easy operation and maintenance. AISHa has been designed to meet the above-cited requirements by means of high field He-free superconducting magnets, while the radial confinement will be provided by a Halbach-type permanent magnet hexapole structure (Figure 1).

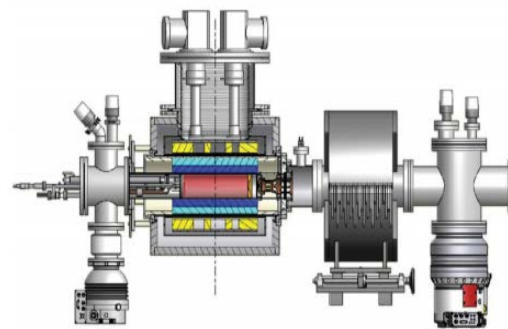


Figure 1: Layout of the AISHa source

After the prototype, now under construction at INFN-LNS in the frame of a partnership with three Italian SME, a second copy will be built for CNAO and discussion about a third one has started.[4]

1.1 Mechanical development

In the development of this new source some improvements of mechanical and structural type have been introduced, in particular the optimization has involved two important parts of the source: the containment chamber and the plasma chamber. The optimization of these components has focused on two aspects: structural mechanics and fluid dynamics; both of these aspects have been optimized by using the COMSOL code.

2. Use of COMSOL Multiphysics

The Finite Element Method approximates a Partial Differential Equations problem with a discretization of the original problem based on a mesh, which is a partition of the geometry into small units of simple shape called mesh elements. The PDE method looks for a solution in the form of a piecewise polynomial function, each mesh element defining the domain for one “piece” of it. Such a piecewise polynomial function will be expressed as a linear combination of a finite set of predefined basis functions. Let us consider for example a 2-dimensional problem with a single dependent variable $p(x,y)$. We would like to solve this problem based on a mesh with quadratic triangular elements. The expression “quadratic elements” refers to the fact that on each mesh element the sought piecewise polynomial function $p^*(x,y)$ is at most a quadratic polynomial. In this case, the solution is expressed as:

$$p(x,y) \cong p^*(x) = \sum_{i=1}^n p_i \varphi_i(x,y)$$

where i refers to a node of the mesh, p_i are the degrees of freedom, $\varphi_i(x,y)$ are the basis functions and n is the total number of nodes, under the assumption that each triangle of the mesh possesses six nodes: three corner nodes and three mid-side nodes [4]. A basis function $\varphi_i(x,y)$ has here the restriction to be a polynomial of degree at most 2 such that its value is 1 at node i and 0 at all other nodes [5]. The degree of freedom p_i is thus the value of $p^*(x,y)$ at node i . The definition of the basis function associated to each node of the mesh can be derived using for

example a general method introduced by Silvester in 1969 [6].

2.1 COMSOL’s Thin-Film Flow Model

All of COMSOL’s single-phase fluid flow interfaces are based on the three fluid dynamics conservation equations known as the Navier-Stokes equations [4], concerning the conservation principles of mass, momentum and energy (Figure 2):

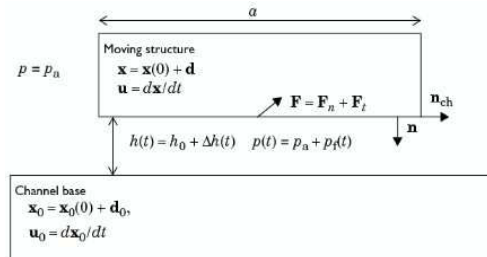


Figure 2: Schematic diagram of the situation to which the thin-Film Flow Model applies

The model that has been used in our simulations is the Thin-Film Flow Model [7] and belongs to the Computational Fluid Dynamics (CFD) module. The Thin-Film Flow Model can be used to model a thin channel of fluid located between two moving structures, as schematized in Figure 2. The upper structure is referred to as the moving structure and the lower one as the channel base. Initially, both structures are surrounded by gas with a constant pressure p_a and the fluid can freely move into and out of the gap. Due to the movements of the structures, an additional and usually time-dependent pressure p_f appears in the gas inside the gap, which produces a normal force \vec{F}_n on the structures. Also a

viscous drag force \vec{F}_t is created which resists the tangential movement of the structure. In the Thin-Film Flow Model, it is however assumed that:

- The film thickness h remains always very small with respect to the dimensions of the solid structures.
- The channel curvature is small.

Also the following assumptions are made:

- The inertial effects in the fluid are negligible compared to the viscous effects, thus the flow is laminar.
- The pressure $p = p_a + p_f$ is constant over the film thickness h .
- The velocity profile over the film thickness is parabolic.
- The fluid is isothermal.

Given these assumptions, solving the fluid flow problem with the Navier-Stokes equations reduces to solving the following equation, called the Reynolds equation:

$$\frac{\partial(p h^3)}{\partial t} + \vec{\nabla}_{tg} \cdot (\rho h \vec{U}) - \rho(\vec{\nabla}_{tg} \Delta h_m \cdot \vec{u}_m - \vec{\nabla}_{tg} \Delta h_b \cdot \vec{u}_b) = 0$$

where ρ is the density, $h = h_0 + \Delta h_m + \Delta h_b$ is the film thickness, t is the time, $\vec{\nabla}_{tg}$ is a gradient computed only with the tangential derivatives along the channel boundaries, U is the mean film velocity, Δh_m and u_m are the normal displacement and the tangential velocity of the so-called “moving structure”, respectively, and Δh_b and u_b are the normal displacement and the tangential velocity of the “channel base”, respectively. The mean film velocity U is actually a function of the pressure p , the dynamic viscosity μ , the film thickness h , the tangential velocities u_m and u_b of the solid structures and the relative flow rate function Q_{ch} that accounts for possible rarefied gas effects:

$$\vec{U} = \frac{\vec{\nabla}_{tg} p}{12\mu} h^2 Q_{ch} + \frac{u_m + u_b}{2}$$

3. Simulation

2.1. First step

Permanent water flow in the plasma chamber is required to provide the expected low temperature. Therefore, the goal of our study was to optimize the design of the groove.

This optimization of the particular was done starting from a model of the chamber used in other sources. The model was designed considering four cylinders: $\varphi = 92$ mm (chamber inner diameter), $\varphi = 94$ mm (water flow internal diameter), $\varphi = 102$ mm (water flow outside diameter) and $\varphi = 104$ mm (chamber external

diameter), each divided in two half cylinders. For each of the two half-cylinders an input, an output and three septa were designed. The domains considered were two, one for water and one for the metal (AISI 316L and aluminum 3003-H18) (Fig. 3).

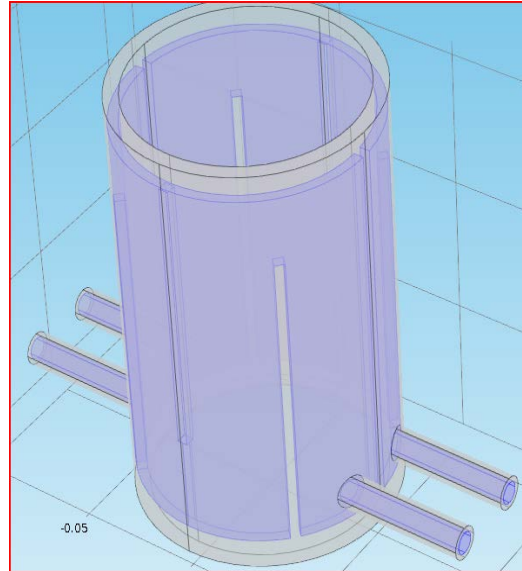


Figure 3. The first model, in gray the metal domain and in purple the water domain.

For the inlet an initial velocity of the water has been determined by requiring a flow rate of 3 liters / minute ($0.00005 \text{ m}^3/\text{s}$) and calculating the section of the input (the input to the diameter is 4 mm so the area is 0.0000502 m^2). From the relation:

$$v = \frac{Q}{A} \quad (1)$$

by substituting the calculated values we obtain that the initial speed has to be 1 m/s. The initial water temperature was set at 20°C .

Concerning the mesh, for both domains we have chosen a tetrahedral mesh. In the domain of the water the choice was to use a mesh more dense than in the domain of the metal.

The results obtained in the case of aluminum 3003-H18 show that the temperature reaches the maximum value of about 300 *K at the output of water, that is, after the water has traveled the half cylinder, it is heated and has lost in part its cooling capacity. Nevertheless, this temperature is satisfactory, as we must have a maximum surface temperature of the lower chamber of 50°C in order not to damage the magnets that are

in contact with it. The flow obtained is substantially laminar. Calculating the Reynolds number with the expression:

$$Re = \frac{v * D}{\mu} \quad (2)$$

and assigning the values: $v=0.35$ m/s (the highest in the flow), $D = 0.004$ mm and assuming the value $1.01 * 10^{-6}$ m²/s for the kinematic viscosity μ of the water, we get a Reynolds number equal to 1386 so we are in the field of laminar flow (Re less than 2300 is laminar flow) (Figures 4 and 5).

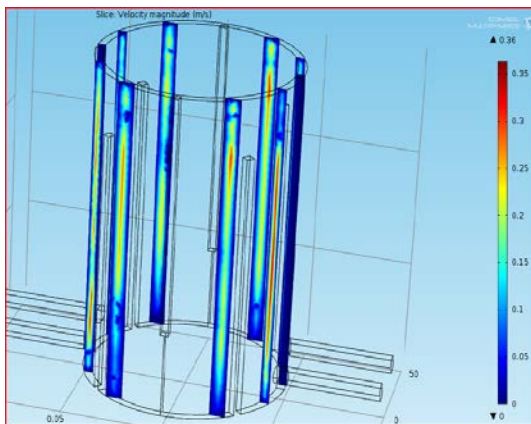


Figure 4. Velocity speed in the aluminum case.

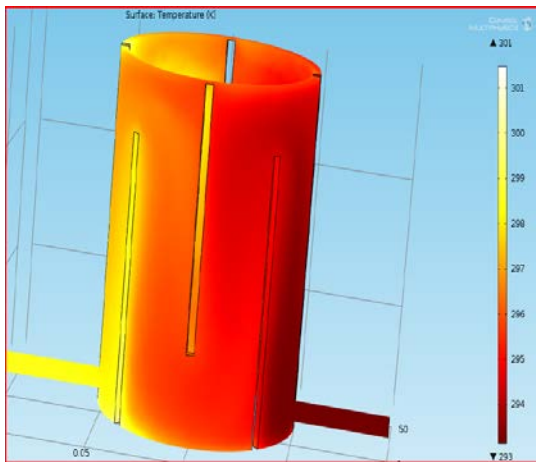


Figure 5. Temperature in the aluminum case.

Subsequently the simulation has been developed using the AISI 316L steel as metal material. The results obtained for the velocity of the water are similar to the case of aluminum, while the maximum temperature reached is lower than in the previous case (Figure 6 and 7).

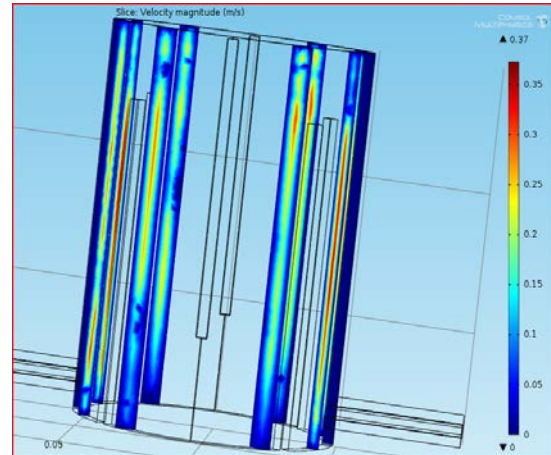


Figure 6. Velocity speed in the aluminum case.

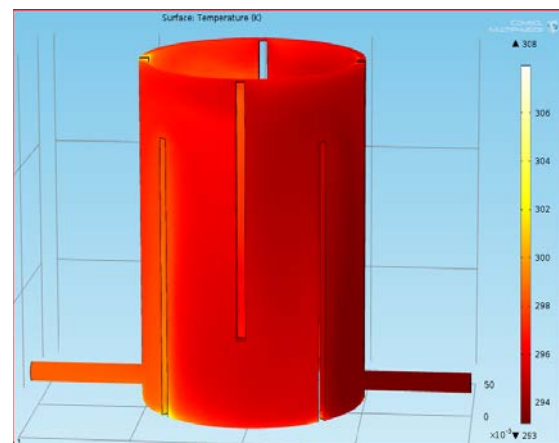


Figure 7. Velocity speed in the aluminum case.

This temperature decrease is due to the characteristics of the two materials: in fact the thermal conductivity of steel (14.6 W/m*K), is lower than that of aluminum (155 W/m*K); it is a measure of the ability of a material to transmit heat (i.e. the lower the value of k, the more insulating is the material).

2.2. Second Step

The first step has been developed using the COMSOL code, considering a length of the chamber of 155 mm. Then the simulation was performed for the actual size of the chamber, that is 655 mm, but as the plasma formation takes place within 360 mm it has been decided to

simplify the simulation, and then the calculations, considering a total length of 360 mm. Another simplification was to divide the plasma chamber into 4 equal sectors each with an input and an output (Figures 8, 9, 10).

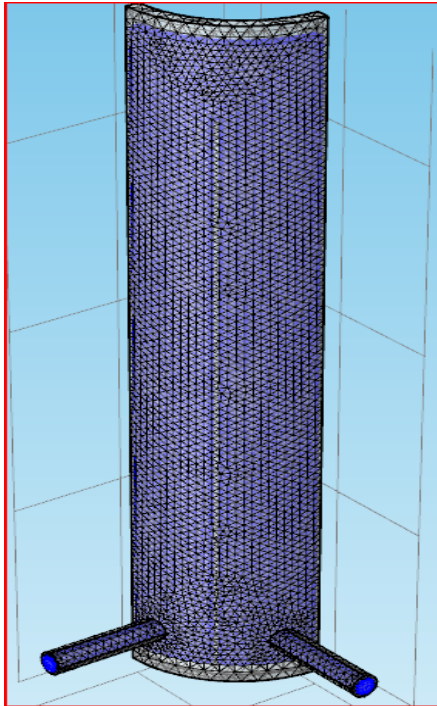


Figure 8. The mesh in the new model

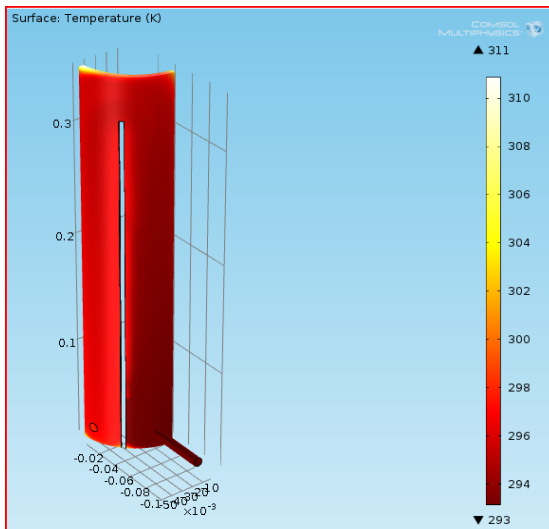


Figure 9. The temperature values in the AISI 316L case.

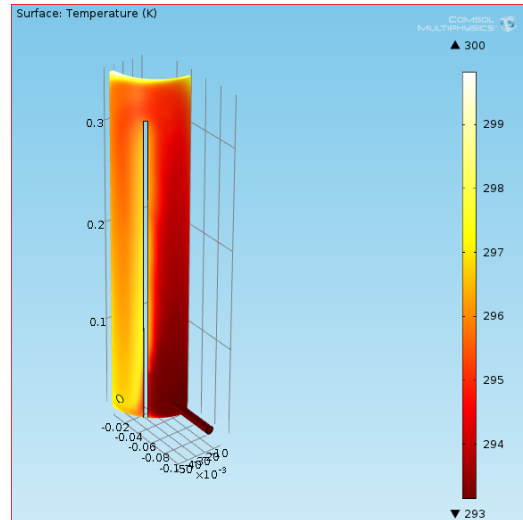


Figure 10. The temperature values in the aluminum 3003-H18 case

An interesting detail is that the Δt between a point near the entrance and a point near the water outlet is about 4°C and the average temperature is 24°C . The maximum temperature of 38°C is on edge (not influential value) as shown in Figure 11a and 11b.

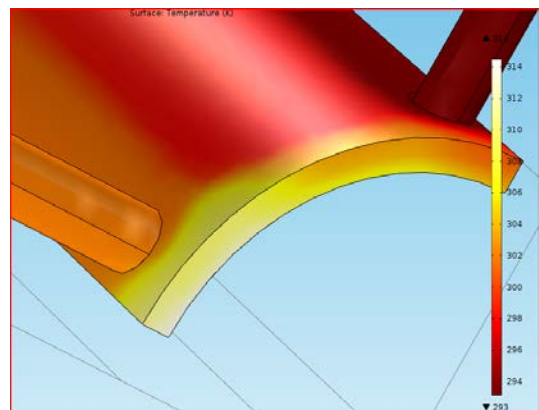


Figure 11a and 11b. The temperature edge.

As in step 1, we have developed the same simulations in the case of another metal material, aluminum 3003-H18.

The results obtained for the water velocity are quite similar to each other (Figure 12).

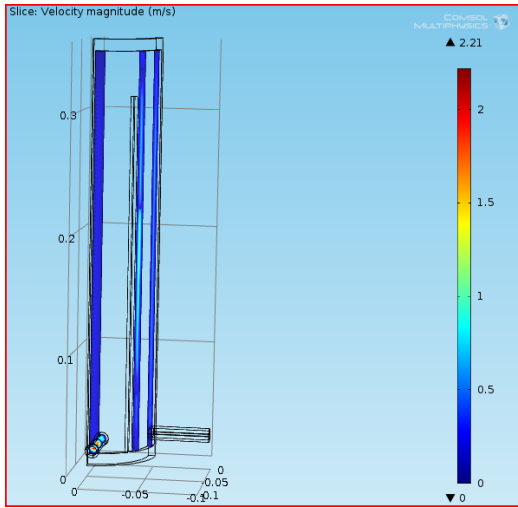


Figure 12. The water velocity values in the aluminum 3003-H18 case

In the plasma chamber the speed values are on average equal to 0.5 m/s and therefore we are in laminar regime as the Reynolds number is about 2000. Pressure drop was calculated using the expressions of both the distributed and concentrated losses. The former is:

$$\Delta p = \rho * \xi * \frac{L}{D} * \frac{v^2}{2} \quad (3)$$

where ρ is the density of water, ξ is the friction factor calculated by means of the Moody (using the Reynolds number and the roughness of the material), L is the length of the chamber, D the diameter of the duct of water (assumed in this case a size of the water domain equal to 4 mm) and v the velocity of water (assumed an average speed of 0.5 m/s from the simulation): the calculation leads to a Δp of about 0.01 bar.

For concentrated losses the expression is:

$$\Delta p = \beta * \rho * \frac{v^2}{2} \quad (4)$$

where ρ is the water density, β is the coefficient of friction equal to 0.5 for the 90-degree elbow and v is the velocity of the water in different cases. The calculation leads to a Δp of about 0.01 bar to the entrance ($v = 2$ m/s); Δp of about 0.002 bar for the output ($v = 0.9$ m/s) and Δp of about 0.0006 bar in the elbows due to the septum ($v = 0.5$ m/s): the sum of all the losses yields a loss of load of 0.023 bar.

5. Conclusions

Our goal was to optimize the design of the plasma chamber. Starting from a simplified model and with subsequent iterations we are able to optimize the plasma chamber of the source AISHa.[8]

6. References

- [1] L. Celona, G. Ciavola, S. Gammino, L. Andò, D. Mascali - DESIGN OF THE AISHA ION SOURCE FOR HADRON THERAPY FACILITIES - Proceedings of ECRIS2012, Sydney, Australia, ISBN ISBN 978-3-95450-123-654
- [2] S. Gammino et al., Rev. Sci. Instrum. 70, 9 (1999), 3577
- [3]. S. Gammino, G. Ciavola, Rev. Sci. Instrum. 71, 2 (2000), 631
- [4] Felippa C.A., Introduction to Finite Element Methods, lecture notes, Department of aerospace engineering sciences of the University of Colorado, Boulder, 2004.
- [5] COMSOL Multiphysics User's Guide v4.1, COMSOL A B, 2010.
- [6] Lewis R.W., Nithiarasu P. & Seetharamu K.N., Fundamentals of the Finite Element Method for Heat and Fluid Flow, New York, John Wiley & Sons, 2004.
- [7] CFD Module User's Guide v4.1, COMSOL AB, 2010.
- [8] L. Celona al. ECR IONS SOURCE DEVELOPMENT AT INFN-LNS – Proceedings of ECRIS2014